This article has been accepted for inclusion in a future issue of this journal. Content is final as presented, with the exception of pagination.



# A Reactive Power Dispatch Strategy With Loss Minimization for a DFIG-Based Wind Farm

Baohua Zhang, *Student Member, IEEE*, Peng Hou, *Student Member, IEEE*, Weihao Hu, *Senior Member, IEEE*, Mohsen Soltani, *Member, IEEE*, Cong Chen, and Zhe Chen, *Senior Member, IEEE*

***Abstract*—An optimal reactive power dispatch strategy is proposed to minimize the total electrical losses of a wind farm (WF), including not only losses in the transmission cables and wind turbine (WT) transformers, but also losses inside wind energy generation systems. The reactive power dispatch inside a WT uses optimal splitting strategy over the stator and the grid side converter (GSC), which aims to minimize the total loss of the wind energy generation system, including the generator, the converters, and the filters. Optimization problems are formulated based on established loss models and WT reactive power limits. A WF is carefully designed and used for case studies. Wake effect is considered when calculating the active power at each WT. The total losses of the WF are calculated by implementing the proposed strategy at different wind speeds and reactive power references. The simulation results show the effectiveness of the proposed strategy.**

***Index Terms*—Doubly fed induction generator, loss minimization, reactive power dispatch, wind farm, wake effect.**

## I. Introduction

WITH increasing integration of wind energy into the power system, Wind Farms (WFs) are required to have the ability to provide reactive power to support the grid [1], [2]. WFs can also provide reactive power to the power system as an ancillary service. One solution for providing reactive power is commissioning additional reactive power compensation sources. However, as Wind Turbines (WTs) with power electronic convertors have the ability to regulate reactive power, it is more economical to utilize the ability of WTs to provide the reactive power ancillary service [3].

The power system operator gives the reactive power reference at the Point of Common Coupling (PCC) of a WF. Then the WF operator calculates and dispatches the required reactive power to each WT. The reactive power dispatch within WFs will affect the efficiency of the whole system, which should be explicitly studied.

The most commonly used dispatch strategy is proportional dispatch, which spreads the required reactive power among all WTs proportional to their available reactive power [4]–[6]. This method is easy to implement and is unlikely to exceed the reactive power limit of each WT. However, it does not consider active power loss in the WF. Another dispatch method proposed in [7]–[9] considers the active power losses along the transmission cables and the transformers of WTs. However, this method does not consider the active power losses in the energy conversion system of WTs, which are responsible for a great part of the total loss in the WFs. Actually, the attempt to minimize active power losses along the transmission cables and the transformers may cause more losses in the energy conversion systems. An optimal dispatch strategy proposed in [10] considered the losses from wind energy conversion systems, transformers and transmission cables, and found an optimal dispatch of reactive power for loss minimization. However, the strategy only used a simple WT control strategy and did not considered the influence of reactive power dispatch inside the Doubly Fed Induction Generator (DFIG) based wind energy generation systems. Since the DFIG energy generation system can regulate reactive power between the stator and the grid side converter (GSC), the reactive power flow inside the system will influence the losses of the system. Therefore the reactive power control method of the DFIG energy generation system should be studied.

The most common method is to provide the reactive power only from the stator side by the rotor side converter (RSC) [11]–[13]. This method can reach good efficiency operating near unity power factor, but the copper losses of the generator will increase significantly when the power factor increases. The second method is to regulate reactive power using both the RSC and the GSC to minimize copper losses [14]–[17]. This method does not consider the losses from the converters and filters. It can reach a lower loss in certain choices of reactive power reference, but will increase the total loss in other cases. [18], [19] proposes a method that splits the reactive power burden over the RSC and the GSC to reach minimum losses for the generator and converters. The splitting ratio is iteratively calculated, forming a set of look-up tables. In the control process, the controller should look up the tables to decide the optimal reactive power currents.

As mentioned above, reactive power optimal dispatch of WFs should consider not only the losses along the transmission system, but also the loss inside the wind energy generation systems, which is related to the control strategy of WTs. The proportional dispatch proposed in [4]–[6] and the transmission loss minimizing dispatch strategy proposed in [7]–[9] both use the most common WT control strategy, which will

Manuscript received August 13, 2015; revised November 01, 2015; accepted December 01, 2015. This work is supported in part by the Danish Strategic Research Center under Grant DSF 09-067255, "Development of a Secure, Economic, and Environmentally-friendly Modern Power System" (SEEMPS) and in part by the Program for Professor of Special Appointment (Eastern Scholar) at Shanghai Institutions of Higher Learning. *(Corresponding author: Weihao Hu.)*

The authors are with the Department of Energy Technology, Aalborg University, Aalborg 9220, Denmark (e-mail: bzh@et.aau.dk; pho@et.aau.dk; whu@et.aau.dk; sms@et.aau.dk; cchen12@googlemail.com; zch@et.aau.dk).

Color versions of one or more of the figures in this paper are available online at http://ieeexplore.ieee.org.

Digital Object Identifier 10.1109/TSTE.2015.2509647

experience higher losses inside WTs than the strategy proposed in [18], [19].

In this paper, an optimal reactive power dispatch strategy is proposed for total loss minimization, which includes not only losses in the transmission cables and WT transformers, but also the losses inside wind energy generation system. The reactive power control of the WT uses optimal splitting strategy over the RSC and the GSC, which is implemented by solving an optimization problem that aims to minimize the total loss from the generator, the converters and the filter. Consequently, reactive power dispatch between the WTs is integrated with the optimal reactive power control strategy of the WTs. The proposed strategy is then compared with traditional dispatch strategies in different cases.

The paper is organized as follows. Section II presents the WF loss models. Section III studies the proportional reactive power dispatch strategies, and Section IV states the formulation of the proposed dispatch strategy. The effect of these strategies are calculated and analyzed in Section V. Finally, the conclusions are in Section VI.

## II. Wind Farm Loss Models

The WTs and the cables are the main devices that cause losses in a WF. The power losses of a WT consist of friction losses in the mechanical part, core losses and copper losses in the DFIG, losses in the converters and the filter, and the losses in the transformer of the turbine. The friction losses and core losses can be considered constant under a certain operation point [17]; therefore they are not considered in this paper. In the following paragraphs, the loss models of each component are derived.

### A. Loss Model of DFIG

For a DFIG operating in a stator voltage oriented reference frame, the steady-state voltage equations are as follows [20]. All variables in the equations are in per unit (pu) system.

$$\begin{bmatrix} V_s \\ 0 \\ V'_{rd} \\ V'_{rq} \end{bmatrix} = \begin{bmatrix} R_s & -X_s & 0 & -X_m \\ X_s & R_s & X_m & 0 \\ 0 & -sX_m & R'_r & -sX'_r \\ sX_m & 0 & sX'_r & R'_r \end{bmatrix} \begin{bmatrix} I_{sd} \\ I_{sq} \\ I'_{rd} \\ I'_{rq} \end{bmatrix} \tag{1}$$

where stator inductance $X_s$ equals $X_{ls} + X_m$, rotor inductance $X'_r$ equals $X'_{lr} + X_m$, $X_{ls}$ is stator leakage inductance, $X_m$ is mutual inductance, $X'_{lr}$ is rotor leakage inductance, *s* is rotor slip. The subscripts are *s*, *r* and *g* for stator, rotor and grid-converter circuits; *l* and *m* for leakage and mutual inductances; *d* and *q* for direct and quadrature axes. The superscript' is used for rotor value referred to the stator.

At a fixed wind speed, the rotor d-axis current is constant, and can be calculated as [20]:

$$I'_{rd} = -\frac{X_s}{V_s X_m}\frac{\omega_s}{\omega_r}P_{mec} \tag{2}$$

$$I_{rd} = uI'_{rd} \tag{3}$$

where $P_{mec}$ is the power extracted from the wind, $\omega_r$ is the angular frequency of the voltages and currents of the rotor windings, $\omega_s$ is the angular frequency of the voltages and currents of the stator windings, *u* is the turns ratio.

The stator q-axis current can be calculated as:

$$I_{sq} = Q_s/V_s \tag{4}$$

where $Q_s$ is the reactive power of the stator.

Deriving from (1), the rotor d-axis current and stator d-axis current can be calculated:

$$I'_{rq} = -AI'_{rd} - \frac{1}{BX_m}I_{sq} - \frac{V_s}{X_m} \tag{5}$$

$$I_{rq} = uI'_{rq} \tag{6}$$

$$I_{sd} = B\left[-X_m I'_{rd} + AX_m I'_{rq} + AV_s\right] \tag{7}$$

where $A = R_s/X_s$, $B = X_s/\left(X_s^2 + R_s^2\right)$.

The copper losses in the DFIG can be calculated using:

$$P_{Cu} = R_s\left(I_{sd}^2 + I_{sq}^2\right) + R_r\left(I_{rd}^2 + I_{rq}^2\right). \tag{8}$$

### B. Loss Model of Converters and the Filter

The losses in the converter, which consists of transistors and reverse diodes, can be divided into switching losses and conducting losses [3], [21]. According to [3], [21], the losses in a converter can be expressed as

$$P_{con}^{loss} = a_l I_{rms} + b_l I_{rms}^2 \tag{9}$$

where $I_{rms}$ is the rms value of the sinusoidal current at the converter ac terminal, and $a_l$ and $b_l$ are the power module constants and can be expressed as

$$a_l = \frac{6\sqrt{2}}{\pi}\left(V_{IGBT} + \frac{E_{ON} + E_{OFF}}{I_{C,nom}}f_{sw} + \frac{E_{rr}}{I_{C,nom}}f_{sw}\right) \tag{10}$$

$$b_l = 3r_{IGBT} \tag{11}$$

where $V_{IGBT}$ is the voltage across the collector and emitter of the IGBT, $E_{ON} + E_{OFF}$ is the total turn-on and turn-off losses of the IGBTs, $I_{C,nom}$ is the nominal collector current of the IGBT, $f_{sw}$is the switching frequency, $E_{rr}$is the turn-off (reverse recovery) loss of the diodes, $r_{IGBT}$ is the lead resistance of the IGBT.

The current flows through Rotor Side Converter (RSC) and GSC can be calculated as:

$$I_{rms}^{RSC} = \sqrt{I_{rd}^2 + I_{rq}^2}$$
$$I_{rms}^{GSC} = \sqrt{I_{gd}^2 + I_{gq}^2}. \tag{12}$$

The grid side converter d-axis current $I_{gd}$ can be calculated:

$$I_{gd} = (I_{rd}V_{rd} + I_{rq}V_{rq})/V_s. \tag{13}$$

The grid side converter q-axis current $I_{gq}$ can be calculated:

$$I_{gq} = Q_g/V_s \tag{14}$$

$$Q_g = Q_{WT} - Q_s \tag{15}$$

This article has been accepted for inclusion in a future issue of this journal. Content is final as presented, with the exception of pagination.



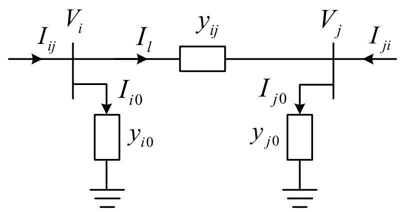


Fig. 1. Cable model for calculating losses [23].

where $Q_g$ is the reactive power provided by the GSC and $Q_{WT}$ is the total reactive power from/to the WT.

With the grid side converter currents, the loss in the grid side filter can be calculated using:

$$P_{filter}^{loss} = R_{filter}\left(I_{gd}^2 + I_{gq}^2\right). \tag{16}$$

So, the total loss from a WT $P_{WT}^{loss}$ is:

$$P_{WT}^{loss} = P_{Cu} + P_{RSC}^{loss} + P_{GSC}^{loss} + P_{filter}^{loss}. \tag{17}$$

### C. Loss Model of Transformers

The active power loss in transformers $P_{trans}^{loss}$ can be calculated using the following equation [22]

$$P_{trans}^{loss} = P_0 + \beta^2 P_k \tag{18}$$

where $\beta$ is the load ratio, $P_0$ is the no-load loss, and $P_k$ is the load loss.

### D. Loss Model of Cables

Consider the cable connecting the two buses *i* and *j* in Fig. 1, where *y* and *I* mean the admittance and current of each cable, and *V* means the voltage on each bus. The cable current, $I_{ij}$, measured at bus *i* and *j* defined positive in the direction $i \rightarrow j$ is given by

$$I_{ij} = I_l + I_{i0} = y_{ij}\left(V_i - V_j\right) + y_{i0}V_i. \tag{19}$$

Similarly, the cable current $I_{ji}$ is given by

$$I_{ji} = -I_l + I_{j0} = y_{ij}\left(V_j - V_i\right) + y_{j0}V_j. \tag{20}$$

The power loss in cable $ij$ is the algebraic sum of the complex powers $S_{ij}$ from bus *i* and *j* and $S_{ji}$ from bus *j* and *i*,

$$S_{ij}^{loss} = S_{ij} + S_{ji} = V_i I_{ij}^* + V_j I_{ji}^*. \tag{21}$$

## III. Traditional Reactive Power Dispatch Strategies

This section introduces the traditional reactive power control strategy for a DFIG WT system and the traditional reactive power dispatch strategies within a WF.

### A. Traditional Reactive Power Control Inside a DFIG WT

The typical configuration of a DFIG WT system is shown in Fig. 2. The output reactive power of the system, $Q_{WT}$, is the combination of reactive power from the stator side of the DFIG, $Q_s$, and reactive power from the GSC, $Q_g$. $Q_s$ and $Q_g$ can be controlled to their reference values $Q_s^{WT}$ and $Q_g^{WT}$ by RSC controller and GSC controller respectively.

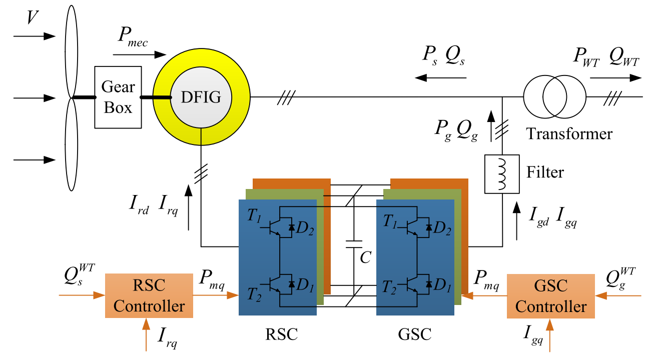


Fig. 2. Typical power flows and reactive power control inside a DFIG WT.

*1) $Q_g^{WT} = 0$:* In traditional WT control strategy, the function of the GSC is to transfer the slip active power from/to the grid to ensure the dc-link voltage constant, so the output reactive power is only controlled by the RSC [12], [24]. The RSC is normally operated by stator voltage oriented vector control, where the *q*-axis current, $I_{rq}$, controls the excitation power. $Q_s$ can be regulated by controlling $I_{rq}$. The reference of $I_{rq}$ can be calculated using (4)–(6) or through a PI controller. In this control concept, $Q_g^{WT}$ equals zero and $Q_s^{WT}$ is equal to $Q_{ref}^{WT}$.

*2) Range of Reactive Power:* The range of the $Q_s$ is determined mainly by two parameters: the rotor side current, $I_r$, and the stator side current, $I_s$ [25]. The rotor side current is usually constrained by the rated RSC current, while the stator side current limit is determined by the thermal limit of the stator conductor [26]. The rated current of the converters is:

$$I_{con}^{rated} = \frac{I_{C,nom}/\sqrt{2}}{1+\delta} \tag{22}$$

where $\delta$ is the safety factor of the converter. The stator current can be calculated using:

$$I_s = \sqrt{I_{sd}^2 + I_{sq}^2}, \tag{23}$$

so the range of $Q_s$ is constrained by

$$I_{RSC}^{rms} \leq I_{RSC}^{rated} \tag{24}$$

$$I_s \leq I_s^{rated} \tag{25}$$

where $I_{RSC}^{rated}$ and $I_s^{rated}$ are the rated currents of the RSC and the stator.

According to the British Grid Code [1], the WFs should be able to provide reactive power ranging from $-0.33$ pu to $+0.33$ pu at the rated active power. Based on the grid code requirement, we calculated $I_s$ under every wind speeds and reactive power references and found the maximum $I_s$ is 0.91 pu. Thus the rated current of the stator, $I_s^{rated}$, is chosen as 0.91 pu. The rotor side converter has the same design as the grid side converter, where the safety factor $\delta$ is chosen as 0.37. Based on the chosen parameters and the parameters in the appendix, the reactive power capability of the DFIG WT system for different stator voltages are shown in Fig. 3. The rotor side current limit is the rated RSC current. The active power and reactive power losses have been considered.

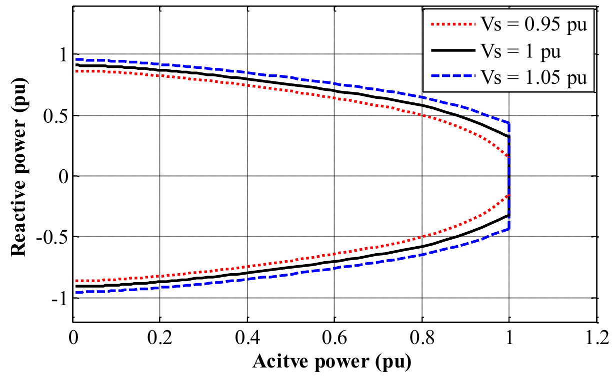


Fig. 3. Capability curve of DFIG for different stator voltages.

### B. Traditional Reactive Power Dispatch Within a WF

*1) Strategy A: Proportional Dispatch::* The strategy dispatches the required reactive power proportionally among all operative generators based on their available reactive power [4]–[6], which can be expressed in (26),

$$Q_{ref}^{WTi} = \frac{Q_{avail}^{WTi}}{\sum_{i=1}^{N_W} Q_{avail}^{WTi}} Q_{ref}^{Total} \tag{26}$$

where $Q_{ref}^{WTi}$ is the reactive power that WT $i$ must generate, $Q_{avail}^{WTi}$ is the available reactive power of WT $i$ in a specific moment, $N_W$ is the number of WTs and $Q_{ref}^{Total}$ is the total reactive power required for all the WTs.

It is worth mentioning that the total reactive power $Q_{ref}^{Total}$ should equal the reactive power requirement of the WFs and the reactive power loss on the cables:

$$Q_{ref}^{Total} = \sum_{k=1}^{N_L} Q_{Cable_k}^{loss} + Q_{ref}^{WF} \tag{27}$$

where $Q_{Cable_k}^{loss}$ is the reactive power loss on cable $k$, $N_L$ is the total number of cables and $Q_{ref}^{WF}$ is the reactive power requirement for the WF. This constraint is implemented by an iterative process [4]. The implementation flow chart of this dispatch strategy is shown in Fig. 4. The available power of each WT is obtained by searching the capability curve, Fig. 3, using the inputs from each WT: the stator voltage $V_s^{WT_i}$ and the mechanical power $P_{mec}^{WT_i}$. The total reactive power $Q_{ref}^{Total}$ is calculated using (27) after a few iteration steps.

*2) Strategy B: WF Transmission Loss Minimization::* This dispatch strategy aims to minimize the transmission losses in the WF, including the active power losses in the transformers and cables [7]–[9]. The WT reactive power reference $Q_{ref}^{WT_i}$ is obtained by solving an optimization problem. This objective function of this optimization can be expressed as:

$$\text{Min} \quad \sum_{i=1}^{N_W} P_{trans_i}^{loss} + \sum_{k=1}^{N_L} P_{Cable_k}^{loss} \tag{28}$$

where $P_{trans_i}^{loss}$ is the active power loss of transformer $i$ and $P_{Cable_k}^{loss}$ is the active power loss of cable $k$.

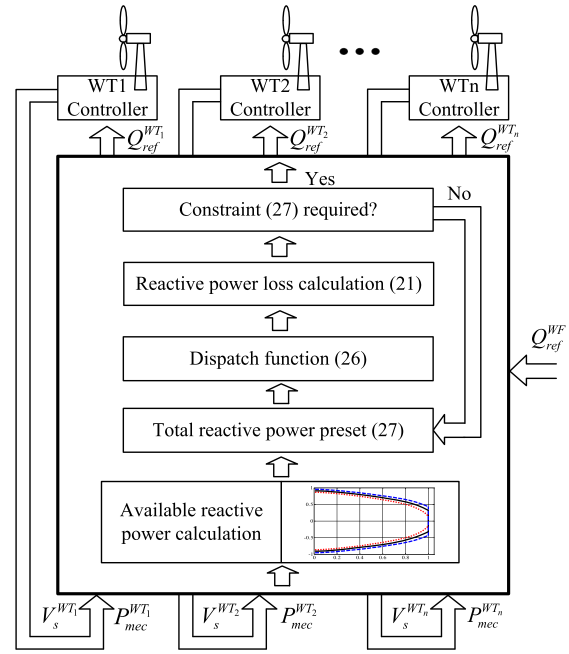


Fig. 4. Implementation of proportional dispatch.

(30)–(32), the voltage constraints of the buses (33), and the reactive power limits of each WT (35), (36).

## IV. Proposed Reactive Power Dispatch Strategy

### A. Optimal Reactive Power Control Inside a DFIG WT

Traditional reactive power control of WTs does not fully use the GSC to regulate reactive power. In the optimal control strategy, the GSC regulates reactive power together with the RSC to minimize the total loss inside the WT. The GSC operates by grid voltage oriented vector control, where *q*-axis current, $I_{gq}$, is varied in order to adjust the reactive power output of the GSC, $Q_g$, which is shown in Fig. 2. The reference value of $I_{rq}$ can be calculated using (14). The references of $Q_s$ and $Q_g$ are obtained by solving the optimization problem in the next sector.

### B. Strategy C: Optimal Reactive Power Dispatch

Comparing to Strategy B, this strategy adds the losses of the WT to the optimization objective. Therefore, it aims to minimize the total active power losses inside the WF, including the losses inside WTs and the losses in the transformers and cables. The optimization variables are the GSC reactive power reference, $Q_g^{WTi}$, and the stator side reactive power reference, $Q_s^{WTi}$, of each WT. The optimization problem can be expressed as follows:

$$\text{Min} \quad \sum_{i=1}^{N_W} \left(P_{trans_i}^{loss} + P_{WT_i}^{loss}\right) + \sum_{k=1}^{N_L} P_{Cable_k}^{loss} \tag{29}$$

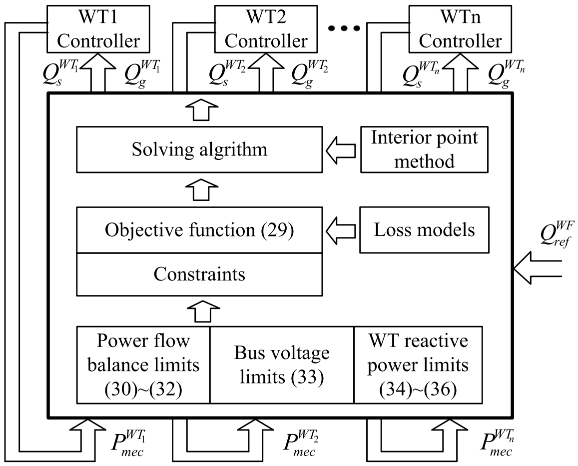


Fig. 5. Flow chart of the optimal dispatch strategy.

s.t.

$$P_j = |V_j| \sum_{i=1}^{N_B} |V_i| |Y_{ji}| \cos(\theta_{ji} - \delta_j + \delta_i) \quad (30)$$

$$Q_j = -|V_j| \sum_{i=1}^{N_B} |V_i| |Y_{ji}| \sin(\theta_{ji} - \delta_j + \delta_i) \quad (31)$$

$$Q_{PCC} = Q_{ref}^{WF} \quad (32)$$

$$V_{\min}^j \le V_j \le V_{\max}^j \quad (33)$$

$$I_{GSC_i}^{rms} \le I_{GSC}^{rated} \quad (34)$$

$$I_{RSC_i}^{rms} \le I_{RSC}^{rated} \quad (35)$$

$$I_s^i \le I_s^{rated} \quad (36)$$

where $P_{WT_i}^{loss}$ is the active power loss from WT $i$, $P_j$ and $Q_j$ are the active power and reactive power injected at bus $j$, $V^j$ is the voltage of each bus, $Y_{ji}$ is the entry in the $j^{th}$ row, $i^{th}$ column of the admittance matrix, $N_B$ is the total number of buses, $Q_{PCC}$ is the reactive power at the point of common connection, and $I_{RSC_i}^{rms}$ and $I_{GSC_i}^{rms}$ can be calculated using (12).

The principle of this strategy is shown in Fig. 5. The inputs are the mechanical power of each WT, $P_{mec}^{WT_i}$ for WT *i*, and the WF reactive power reference, $Q_{ref}^{WF}$. The outputs are $Q_g^{WTi}$ and $Q_s^{WTi}$ for each WT *i*. The objective function (29) can be obtained from the loss models established in Section II. Constraints include the power flow balance limits (30)–(32), bus voltage limits (33), and reactive power limits (34)–(36). In this paper, the voltage range is assumed to be [0.95; 1.05]. The optimization problem is solved by using interior-point methods [27].

As can be seen, each WT should receive two references from the WF controller: $Q_g^{WTi}$ and $Q_s^{WTi}$. This is quite different from the traditional control scheme of WTs. The two control variables should be regulated separately by the GSC and the RSC.

## V. Case Study

In this paper, a WF which has 5 rows with 5 turbines each row is chosen to test the proposed strategy. The WF is laid out in a rectangular pattern with 882 m between the turbines. The layout of the WF is shown in Fig. 6.

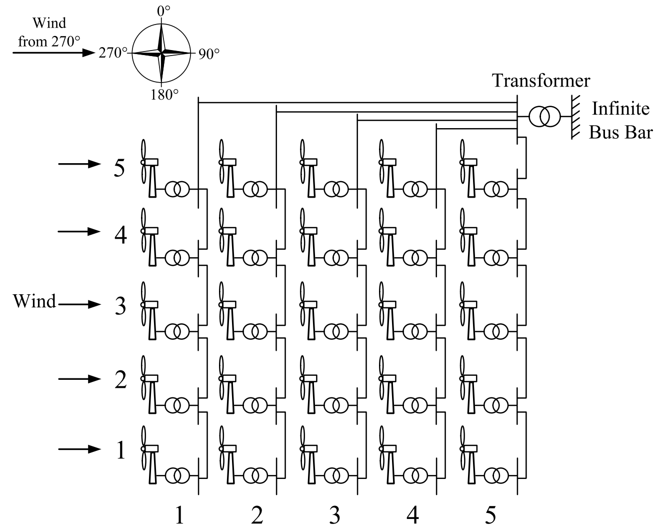


Fig. 6. The layout of the wind farm.

TABLE I
Parameters of Cables [28]

| Cross section mm2 | Resistance Ω /km | Capacitance μF/km | Inductance mH/km |
|---|---|---|---|
| 95 | 0.1842 | 0.18 | 0.44 |
| 150 | 0.1167 | 0.21 | 0.41 |
| 240 | 0.0729 | 0.24 | 0.38 |

TABLE II
The Wind Velocity at the WTs in Each Row

| Column | 1 | 2 | 3 | 4 | 5 |
|---|---|---|---|---|---|
| Wind velocity (m/s) | 10 | 7.8 | 7.5 | 7.49 | 7.39 |

The cables in the WF are 95, 150 or $240\,\text{mm}^2$ (chosen by load, corresponding to cables between row 1 and row 3, between row 3 and row 5 and between row 5 and the transformer, respectively) XLPE-Cu, operated at 34 kV nominal voltage [28]. The parameters of the cables are shown in Table I. The WT system parameters are presented in the Appendix.

### A. Scenario I: $V = 10m/s$, $Wind\ Direction = 270°$

The dispatch of reactive power is strongly related to the distribution of the active power. In this paper, WTs were controlled using a traditional active power control strategy, which can be represented by a power curve. The Jensen model is used to calculate the wake expanding behind the upstream WT [29], [30]. The wind velocity at downstream WTs is calculated using the method proposed in [31].

In this scenario, the incoming wind of the WF has a velocity of 10 m/s and direction of 270°. After calculation with the wake model, the wind velocity at the WTs in each row is as listed in Table II. Based on the wind velocity and traditional WT active power control strategy, the total WF power extracted from the wind is 49.8 MW.

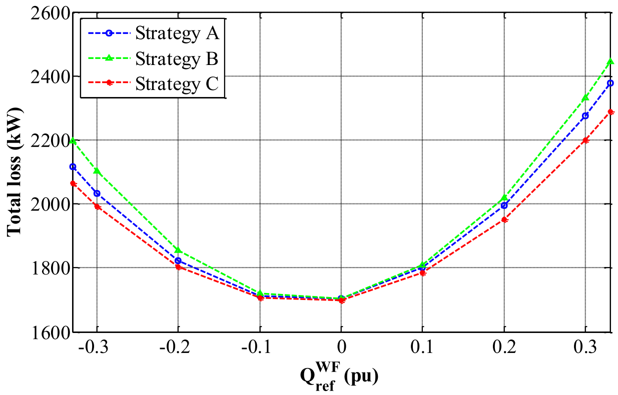


Fig. 7. The total losses in the WF using different dispatch strategies.

TABLE III
LOSSES IN DIFFERENT WF COMPONENTS USING DIFFERENT DISPATCH STRATEGIES

| WF Losses (kW) \ $Q_{ref}^{WF}$ (pu) | | -0.33 | -0.3 | -0.2 | -0.1 | 0 | 0.1 | 0.2 | 0.3 | 0.33 |
|---|---|---|---|---|---|---|---|---|---|---|
| A | Cable+Transformers | 718 | 695 | 634 | 597 | 584 | 594 | 628 | 686 | 707 |
| | Turbine | 1398 | 1339 | 1188 | 1114 | 1121 | 1207 | 1365 | 1591 | 1671 |
| | Total | 2116 | 2033 | 1821 | 1711 | 1705 | 1801 | 1994 | 2276 | 2378 |
| B | Cable+Transformers | 702 | 682 | 628 | 595 | 584 | 593 | 623 | 674 | 694 |
| | Turbine | 1495 | 1421 | 1228 | 1125 | 1121 | 1215 | 1397 | 1658 | 1750 |
| | Total | 2197 | 2103 | 1856 | 1720 | 1705 | 1808 | 2020 | 2332 | 2444 |
| C | Cable+Transformers | 712 | 690 | 629 | 593 | 580 | 591 | 624 | 681 | 702 |
| | Turbine | 1354 | 1303 | 1175 | 1113 | 1119 | 1193 | 1328 | 1520 | 1588 |
| | Total | 2066 | 1993 | 1805 | 1706 | 1700 | 1783 | 1953 | 2201 | 2289 |

The total losses using different reactive power dispatch strategies are shown in Fig. 7. The range of reactive power reference values for the WF is $-0.33$ to 0.33, which is the requirement of the British Grid Code [1]. It is clear that the proposed strategy, Strategy C, can ensure the WF produces the least total loss. Strategy B brings the most total loss, though it aims to minimize the losses in the transmission cables and transformers. The advantage of Strategy C is more obvious when the absolute value of the reference reactive power for the WF, $Q_{ref}^{WF}$, is bigger.

In order to find the main reason for the benefits of Strategy C, we calculated the losses in each component of the WF using strategies A, B and C, which are given in Table III. It is clear that by using Strategy B, the losses in cables and transformers are the lowest, but the losses on wind turbines are the highest, which means minimizing the losses in cables will increase losses from the wind turbines and transformers. Comparatively, the losses in cables and transformers using Strategy C is higher than that of using Strategy B. However, the losses in wind turbines decrease significantly using Strategy C, which makes the total loss minimal. The losses in cables and transformers using Strategy A are always the highest, whereas the losses from wind turbines are much lower than with Strategy B. Thus the total loss using Strategy A is still lower than that using Strategy B.

It also can be observed that the total loss when $Q_{ref}^{WF}$ is positive is higher than the loss when $Q_{ref}^{WF}$ is negative, even though the absolute value of $Q_{ref}^{WF}$ is the same. The reason for this is that the losses in a WT are minimal when they absorb a certain amount of reactive power for excitation, which can refer to [32]. Therefore, when $Q_{ref}^{WF}$ is negative, the total loss from WTs is relatively small.

TABLE IV
TOTAL LOSSES FORM THE WF USING DIFFERENT DISPATCH STRATEGIES FOR DIFFERENT WIND DIRECTIONS

| WF Loss (kW) \ $Q_{ref}^{WF}$ (pu) | | -0.33 | -0.3 | -0.2 | -0.1 | 0 | 0.1 | 0.2 | 0.3 | 0.33 |
|---|---|---|---|---|---|---|---|---|---|---|
| A | 0° | 2043 | 1959 | 1744 | 1633 | 1627 | 1725 | 1921 | 2208 | 2311 |
| | 90° | 2060 | 1976 | 1761 | 1649 | 1643 | 1741 | 1937 | 2224 | 2327 |
| | 180° | 2083 | 2001 | 1789 | 1680 | 1674 | 1771 | 1964 | 2247 | 2349 |
| | 270° | 2116 | 2033 | 1821 | 1711 | 1705 | 1801 | 1994 | 2276 | 2378 |
| B | 0° | 2083 | 1987 | 1766 | 1636 | 1627 | 1726 | 1926 | 2236 | 2334 |
| | 90° | 2107 | 2008 | 1767 | 1652 | 1643 | 1741 | 1939 | 2243 | 2362 |
| | 180° | 2165 | 2070 | 1807 | 1684 | 1674 | 1776 | 1980 | 2307 | 2420 |
| | 270° | 2196 | 2102 | 1844 | 1717 | 1705 | 1801 | 2010 | 2332 | 2444 |
| C | 0° | 1986 | 1913 | 1727 | 1631 | 1625 | 1710 | 1879 | 2127 | 2216 |
| | 90° | 2002 | 1930 | 1744 | 1647 | 1641 | 1726 | 1895 | 2143 | 2232 |
| | 180° | 2037 | 1964 | 1777 | 1679 | 1673 | 1757 | 1927 | 2176 | 2264 |
| | 270° | 2070 | 1997 | 1808 | 1710 | 1703 | 1787 | 1956 | 2208 | 2293 |

### *B. Scenario II: $V = 10m/s$, $Wind\ Direction = 0°, 90°$ and 180°*

When the wind direction is 0°, 90° and 180°, the total losses in the WF using different control strategies are shown in Table IV. As the wind farm is square, the total WF power extracted from the wind should be the same in this scenario, which is 49.8 MW. At all set points for wind direction and WF reactive power, the total losses using strategy C are the lowest, while the total losses using strategy B are the highest.

The total losses with wind direction 0° are always the lowest, whereas the total losses with wind direction 270° are always the highest. The explanation for this is that when the wind direction is 0°, the WTs with higher wind speed are nearer to the PCC, so the active power circulation distance is smaller, resulting in lower losses in cables.

### *C. Scenario III: $V = 10m/s$, $Q_{ref}^{WF} = 0.3\,pu$*

The wakes at directions 0°, 90°, 180° and 270° have the same pattern because the WF is square and the distances between WTs are the same. Therefore, the effect of the proposed strategy should be evaluated for other wind directions. In this case, wind directions ranging from 180° to 270° at 10° intervals are chosen, with wind velocity of 10 m/s and $Q_{ref}^{WF}$ at 0.3 pu. In this range, wind blows more frequently in a year. The total WF power extracted from the wind at each wind direction is shown in Fig. 8.

The comparisons of these strategies are shown in Fig. 9. The legend "A–C" means the reduction of losses from Strategy C relative to Strategy A. A similar meaning applies for "B–C". It can be seen that the total losses using Strategy C are always

This article has been accepted for inclusion in a future issue of this journal. Content is final as presented, with the exception of pagination.



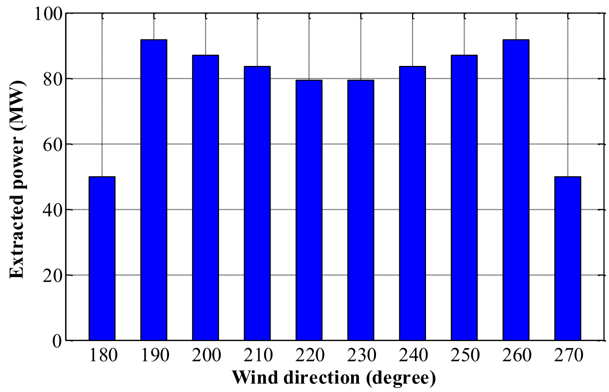


Fig. 8. The total extracted wind power of the WF at each wind direction.

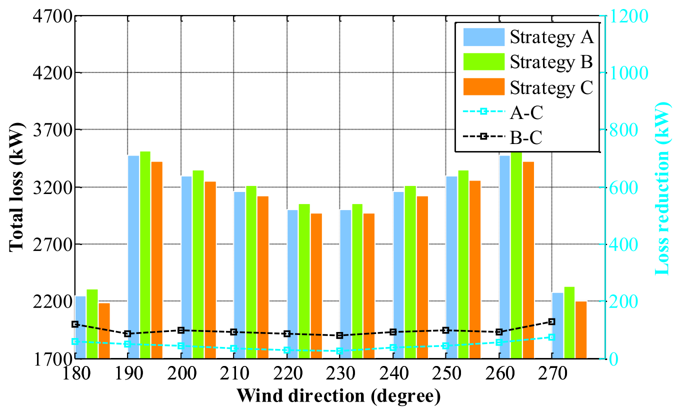


Fig. 9. The total loss using these strategies and the loss reduction using Strategy C at different wind directions.

the lowest, while those using Strategy B are always the highest. The total losses in directions 180° and 270° are lower than those in other wind directions. The reason is that the wake effect in directions 180° and 270° is stronger, so wind power at downwind WTs is lower, which lead to reduced losses in the WF. However, the loss reduction in directions 180° and 270° is higher than that in other directions. That is also a result of the wake effect. The active power at each WT inside the WF is more diverse in these wind directions, therefore the current inside the WTs is more diverse. As shown in section II, the losses in a WT are almost proportional to the square of the current flowing inside, so the total losses from WTs inside the WF is bigger when the currents are more diverse. This brings more space for reducing the total loss to the optimal dispatch of reactive power.

### D. Scenario IV: $Wind\ Direction = 270°$, $Q_{ref}^{WF} = 0.3\ pu$

In this scenario, these strategies are evaluated under different wind velocities. The wind velocity varies from 5 m/s to 14 m/s. The reason for this choice is that when wind velocity is under 5 m/s, the wind speed at some downwind WTs is below the cut-in wind speed, while the wind speed at all WTs exceeds the rated wind speed when wind velocity is higher than 14 m/s. The total WF power extracted from the wind at each wind speed is shown in Table V. The total losses and loss reductions are shown in Fig. 10. The total losses using Strategy C are always the lowest, while the total losses using Strategy B are always the

TABLE V
THE TOTAL EXTRACTED WIND POWER OF THE WF AT EACH WIND SPEED

| Wind speed (m/s) | 5 | 6 | 7 | 8 | 9 | 10 | 11 | 12 | 13 | 14 |
|---|---|---|---|---|---|---|---|---|---|---|
| Extracted Power (MW) | 3 | 7 | 15 | 24 | 36 | 50 | 67 | 88 | 115 | 125 |

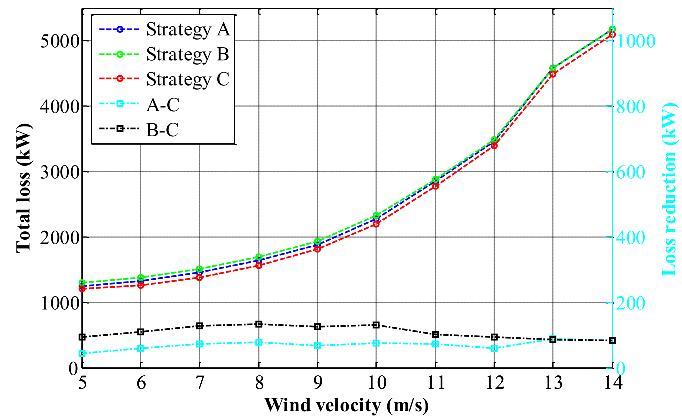


Fig. 10. The total loss using these strategies and the loss reduction with respect to Strategy C at different wind velocities.

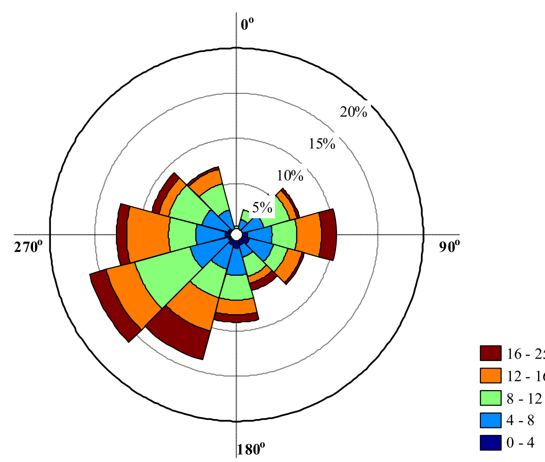


Fig. 11. Wind rose for the wind climate in the vicinity of FINO3.

highest. The loss reduction varies with wind velocity. The greatest loss reduction happens when the wind velocity is 8 m/s. The reason is the variation in wind speed between WTs is stronger at this wind velocity.

### E. Scenario V: Total WF Loss in a Year

As the total loss saving varies with wind velocity and wind direction, it is necessary to evaluate the effectiveness of the proposed strategy over the course of a year. The wind data is obtained from the Norwegian Meteorological Institute [33]. The wind speeds are sampled per every 3 hours, and then averaged over each day. The wind data can be expressed with a wind rose with a 30° direction interval, as shown in Fig. 11.

The total wind power captured by the WTs and the total losses using these strategies are calculated separately with the data from the wind rose, assuming the WTs are available over

TABLE VI
TOTAL LOSSES IN THE WF OVER A YEAR USING DIFFERENT WF DISPATCH STRATEGIES

| Loss (pu) (GWh) \ $Q_{ref}^{WF}$ | -0.33 | -0.3 | -0.2 | -0.1 | 0 | 0.1 | 0.2 | 0.3 | 0.33 |
|---|---|---|---|---|---|---|---|---|---|
| A | 26.10 | 25.42 | 23.65 | 22.71 | 22.65 | 23.43 | 24.98 | 27.25 | 28.07 |
| B | 26.47 | 25.75 | 23.79 | 22.75 | 22.65 | 23.45 | 25.08 | 27.51 | 28.35 |
| C | 25.70 | 25.10 | 23.53 | 22.69 | 22.63 | 23.32 | 24.68 | 26.67 | 27.38 |
| A–C | 0.41 | 0.32 | 0.12 | 0.01 | 0.02 | 0.11 | 0.30 | 0.58 | 0.69 |
| B–C | 0.77 | 0.65 | 0.26 | 0.06 | 0.02 | 0.13 | 0.40 | 0.83 | 0.98 |

the whole year. Results are listed in Table VI. Total captured wind power is 618.51 GWh and the total losses over a year at different $Q_{ref}^{WF}$ are given in Table V. Comparing with Strategy A and Strategy B, Strategy C saves a large amount of wind power at every $Q_{ref}^{WF}$ set point. The largest saving with respect to Strategy B is 0.98 GWh when the WF is operating at $Q_{ref}^{WF} = 0.33$ pu for the whole year.

## VI. CONCLUSION

An optimal reactive power dispatch strategy is developed in this paper to minimize the total losses from every device in the WF, including the generators, converters, filters, transformers and cables. The optimization problem considers the power balance equality constraints, the voltage and angle limits on the buses, and reactive power limit of the WTs. Two traditional strategies were compared with the proposed strategy and the results show the effectiveness of the proposed strategy. The proposed strategy can be used in WF energy management systems or wind power dispatch centers. The implementation of this optimized strategy requires a modification on the WT control level, i.e., each WT should be able to follow two reactive power references by controlling the RSC and the GSC. Further development for this dispatch strategy will be to add an optimized active power dispatch strategy in order to maximize the total active power output.

## APPENDIX

### A. Wind Turbine

The 5 MW NERL WT is adopted as the reference WT [34]. The parameters are shown in Table VII.

TABLE VII
NERL 5 MW WIND TURBINE SPECIFICATION [34]

| Parameter | 5 MW NERL Wind Turbine |
|---|---|
| Cut-in, Rated, Cut-out Wind Speed | 3 m/s, 11.4 m/s, 25m/s |
| Rotor, Hub Diameter | 126 m, 3m |
| Rated Power | 5 MW |
| Cut-In, Rated Rotor Speed | 6.9 rpm, 12.1 rpm |
| Gearbox ratio | 97:1 |

### B. Converters

The IGBT module ABB 5SNA 2000K451300 is chosen. Based on the data for the IGBT module on the data sheet [35], the power module constants $a_l = 7.0252$ and $b_l = 0.0087$, and $f_{sw}$ is chosen as 800 Hz.

### C. Transformer

The Siemens GEAFOL cast-resin transformer is chosen as the transformer set in the WT [36]. The transformer is rated at 8000kVA, with no-load loss of 13.5 kW and load loss of 36 kW.

### D. DFIG [37]

The parameters are listed in Table VIII.

TABLE VIII
PARAMETERS OF 5MW DIFG

| Parameters | Value | Per unit value |
|---|---|---|
| Rated Mechanical Power | 5MW | 1.0 pu |
| Rated Stator Phase Voltage | 548.48 V (rms) | 1.0 pu |
| Rated Stator Frequency | 50 Hz | 1.0 pu |
| Rated Rotor Speed | 1170 rpm | 1.0 pu |
| Nominal Rotor Speed Range | 670-1170 rpm | 0.573-1.0 pu |
| Rated Slip | -0.17 | |
| Number of Pole Pairs | 3 | |
| Stator Winding Resistance, $R_s$ | 1.552 mΩ | 0.0086 pu |
| Rotor Winding Resistance, $R_r$ | 1.446 mΩ | 0.008 pu |
| Stator Leakage Resistance, $L_{ls}$ | 1.2721 mH | 2.2141 pu |
| Rotor Leakage Resistance, $L_{lr}$ | 1.1194 mH | 1.9483 pu |
| Magnetizing Inductance, $L_m$ | 5.5182 mH | 9.6044 pu |
| Base Current, $I_B$ | 3038.7 A (rms) | 1.0 pu |
| Base Impedance, $Z_B$ | 0.1805 Ω | 1.0 pu |

## REFERENCES


[1] National Grid plc. (2015, Jan.). *The Grid Code* (issue 5, revision13) [Online]. Available: http://www.nationalgrid.com/uk

[2] Energinet. (2010, Sep.). *Technical Regulation 3.2.5 for Wind Power Plants with a Power Output Greater Than 11 kW* (revision 4.1) [Online]. Available: http://www.energinet.dk

[3] N. R. Ullah, K. Bhattacharya, and T. Thiringer, "Wind farms as reactive power ancillary service providers—Technical and economic issues," *IEEE Trans. Energy Convers.*, vol. 24, no. 3, pp. 661–672, Sep. 2009.

[4] A. Tapia, G. Tapia, and J. X. Ostolaza, "Reactive power control of wind farms for voltage control applications," *Renew. Energy*, vol. 29, pp. 377–392, 2004.

[5] Y. Lang, X. Zhang, D. Xu, H. F. Ma, and S. R. Hadianmrei, "Reactive power analysis and control of doubly fed induction generator wind farm," *Proc. CSSE*, vol. 27, no. 9, Mar. 2007, pp. 77–82.

[6] J. R. Saenz, A. Tapia, G. Tapia, F. Jurado, X. Ostolaza, and I. Zubia, "Reactive power control of a wind farm through different control algorithms," in *Proc. 4th IEEE Int. Conf. Power Electron. Drive Syst.*, Denpasar, Indonesia, 2001, pp. 203–207.

[7] R. G. De Almeida, E. D. Castronuovo, and J. A. Peas Lopes, "Optimum generation control in wind parks when carrying out system operator requests," *IEEE Trans. Power Syst.*, vol. 21, no. 2, pp. 718–725, May 2006.

[8] B. Kanna and S. N. Singh, "Towards reactive power dispatch within a wind farm using hybrid PSO," *Int. J. Elect. Power Energy Syst.*, vol. 69, pp. 232–240, 2015.

[9] M. Martinez-Rojas *et al.*, "Reactive power dispatch in wind farms using particle swarm optimization technique and feasible solutions search," *Appl. Energy*, vol. 88, no. 12, pp. 4678–4686, 2011.

[10] B. Zhang, W. Hu, P. Hou, and Z. Chen, "Reactive power dispatch for loss minimization of a doubly fed induction generator based wind farm," in *Proc. IEEE 17th Int. Conf. Elect. Mach. Syst. (ICEMS'14)*, Hangzhou, China, 2014, pp. 1373–1378.